Biomimetic hydrogel derived from decellularized dermal matrix facilitates skin wounds healing

Yaling Yu [a,b,1], Huimin Xiao [a,c,1], Guoke Tang [d,1], Hongshu Wang [a], Junjie Shen [a], Yi Sun [a], Shuaiqun Wang [e], Wei Kong [e], Yimin Chai [a,**], Xuanzhe Liu [a,***], Xing Wang [f,g,*], Gen Wen [a,****]

[a] Department of Orthopedic Surgery, Shanghai Sixth People's Hospital Affiliated to Shanghai Jiao Tong University School of Medicine, Shanghai, 200233, China
[b] Institute of Microsurgery on Extremities, Shanghai Sixth People's Hospital Affiliated to Shanghai Jiao Tong University School of Medicine, Shanghai, 200233, China
[c] College of Fisheries and Life Science, Shanghai Ocean University, Shanghai, 201306, China
[d] Department of Orthopedics, Shanghai General Hospital, Shanghai Jiaotong University, Shanghai, 200080, China
[e] College of Information Engineering, Shanghai Maritime University, Shanghai, 201306, China
[f] Beijing National Laboratory for Molecular Sciences, Institute of Chemistry, Chinese Academy of Sciences, Beijing, 100190, China
[g] University of Chinese Academy of Sciences, Beijing, 100049, China

ARTICLE INFO

ABSTRACT

Cutaneous wound healing affecting millions of people worldwide represents an unsolvable clinical issue that is frequently challenged by scar formation with dramatical pain, impaired mobility and disfigurement. Herein, we prepared a kind of light-sensitive decellularized dermal extracellular matrix-derived hydrogel with fast gelling performance, biomimetic porous microstructure and abundant bioactive functions. On account of its excellent cell biocompatibility, this ECM-derived hydrogel could induce a marked cellular infiltration and enhance the tube formation of HUVECs. *In vivo* experiments based upon excisional wound splinting model showed that the hydrogel prominently imparted skin wound healing, as evidenced by notably increased skin appendages and well-organized collagen expression, coupled with significantly enhanced angiogenesis. Moreover, the skin regeneration mediated by this bioactive hydrogel was promoted by an accelerated M1-to-M2 macrophage phenotype transition. Consequently, the decellularized dermal matrix-derived bioactive hydrogel orchestrates the entire skin healing microenvironment to promote wound healing and will be of high value in treatment of cutaneous wound healing. As such, this biomimetic ddECMMA hydrogel provides a promising versatile opinion for the clinical translation.

1. Introduction

Critical-sized full thickness cutaneous defect resulting from burns, acute and chronic wounds is an unsolvable clinical problem affecting millions of people worldwide, constituting an enormous and escalating economic burden on individual patients and society [1]. Skin wound healing in adults is distinct from prenatal wound healing that re-capitulates the original skin architecture, and always results in scar formation with dramatical pain, impaired mobility and disfigurement, thus reducing quality of life, representing major challenges for medicine and even cosmetics [2]. Though the booming development of skin tissue engineering, there still remains several obstacles to realizing scar-free wound healing, including poor vascularization, interfered re-epithelization, abnormal scar formation, etc. [3]. Thus, to improve the quality of adult skin wound healing, engineered biomaterials should not only have suitable topographical cues to repair the skin defects, but also provide bioactive components to ensure efficient skin regeneration.

Accumulated researches have provided evidence that extracellular matrix (ECM) components that provoke cellular adhesion, proliferation and differentiation are instrumental to augmenting scar-free wound healing [4]. Although many attempts have applied ECM components for skin tissue engineering applications [5], the reductionist biochemical

---

components, lacking diversity of biological components, are significantly limited to achieve complete tissue regeneration [4a]. Decellularized extracellular matrix scaffolds (dECM), three-dimensional natural biomaterials harvested by removal of cellular components without altering intrinsic ECM structure and components, are ideally assembled with variety of biological active components, including proteoglycans, growth factors, cytokines, and adhesive proteins, and featured by satisfactory biocompatibility, non-immunogenicity and easy accessibility [6]. These advantages render dECM to be one of the most promising ECM-mimetic materials in translational medicine [7]. In our previous work, we have demonstrated the effectiveness of kidney and nail bed-derived dECM scaffolds in promoting tissue and organ regeneration [8]. However, main disadvantages of unchangeable physical morphology and low structural integrity limite their further applications in person specialized medicine [9]. Thus, in present-day biomaterial research, there is an urgent need for modification of dECM to be a merger of both biologically active and physiochemically tailorable biomaterials.

Due to physiochemical tailorability, shape fidelity, and printability, dECM-based hydrogels, derived from adipose, dermal, and amniotic membrane, have been extensively employed for promoting cutaneous wound healing recently [10]. These dECM hydrogels are thermosensitive, with gelation occurred at around 37 °C, while the reversible thermo-responsibility restricts their application *in vivo* to some extent due to the gel-sol transition during decreased temperature. Comparatively, irreversible, photo-crosslinked hydrogel responsive to light is more attractive. In addition, the application of mixing of dECM thermosensitive hydrogels with other cross-linking systems (e.g., dECM/fibrinogen, dECM/GelMA) has also been attempted [8d,11]. However, these methods are still limited because the unaccessibility of source material (such as amniotic membrane) and the mixing of other crosslinked hydrogels will inevitably lead to inaccurate simulation of ECM composition and proportions in the skin's native microenvironment, thus initiating imperfect skin wound healing.

In the study conducted herein, we applied the accessible porcine dermal-derived dECM materials to fabricate a covalently crosslinked dermal ECM hydrogel (ddECMMA) through the amide bond reaction between methacryloyl groups and amino functional groups under the excitation of ultraviolet light. The ddECMMA hydrogel, without interfering with the composition and proportion of natural skin ECM, could simulate the complexity of skin's natural microenvironment and possess the physiochemical adjustability and high cellular activity to promote the repair of full-thickness skin defects (Scheme 1). We discovered that the

ddECMMA hydrogel activated SOX9-positive hair follicle stem cells, prompted the development of hair follicles, and facilitated scarless wound healing coupled with significantly enhanced angiogenesis. The cell analysis of multi-parameter flow cytometry, as well as the measurement of gene expression, provided evidence that acceleration of M1-to-M2 macrophage transition by ddECMMA hydrogel could elicit scarfree skin regeneration.

2. Results and discussion

2.1. Characterization of ddECM scaffold and ddECMMA hydrogel

Considering that porcine skin has impressive similarities to the human skin in general structure, thickness, collagen, lipid composition and hair follicle content [12], the ddECM scaffold in this study was manufactured from porcine skin to become porcelain white with soft texture (Fig. 1A). Deoxyribo nucleic acid (DNA) content was nearly undetectable in the ddECM scaffold, compared with that in the native tissue, the residual amount of DNA was lower than the minimum standard for decellularized scaffolds (50 ng mg^{-1}) [13,14] (Fig. 1B). Besides, there was no obvious nuclear compositions observed in the ddECM tissues, depicted in the hematoxylin-eosin (H&E) staining. Alongside with the observations in the H&E staining, Masson's trichrome staining showed that the histological structure of ECM was intactly preserved post decellularization procedure, including microvascular structure and collagen arrangement (Fig. 1C). Detailed investigations on ECM microstructure by scanning eletron microscope (SEM) scanning revealed a similar unbroken ECM microstructure (Fig. 1D). As indicated by several researches, collagen I, elastin and laminin are major constituents making up the dermal ECM [15], the visualization of these ECM elements before and post the decellularization was conducted by the immunofluorescent staining. As shown in Fig. 1E, these proteins were well retained in the post-decellularized ddECM scaffolds.

Despite of the perfect decellularization of ddECM scaffold, the unchangeable physical morphology and low structural integrity limited its further application in person specialized medicine. In this study, to enhance the physiochemical tailorability and structural integrity, the ddECM scaffold was modified into the photo-crosslinkable hydrogel by the high-efficiently chemical reaction with methacrylic anhydride (MA) and amino groups within the ddECM (ddECMMA), as depicted in Fig. 2. The deformation behavior of ddECMMA precursor solution occurred under the ultraviolet in the presence of photoinitiator of Irgacure 2959
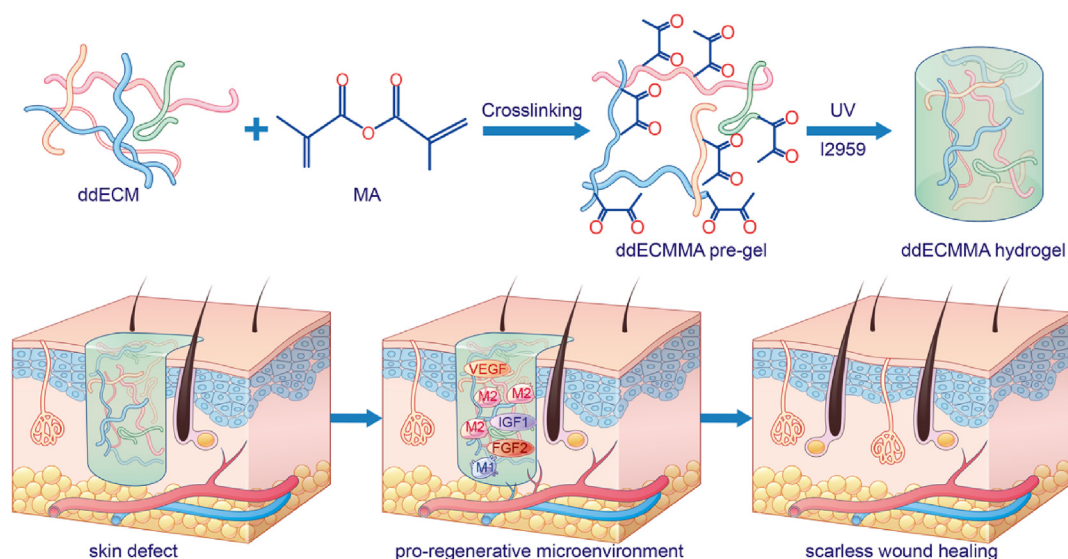
Scheme 1. Schematic illustration of the ddECMMA hydrogel for the scarless wound healing.
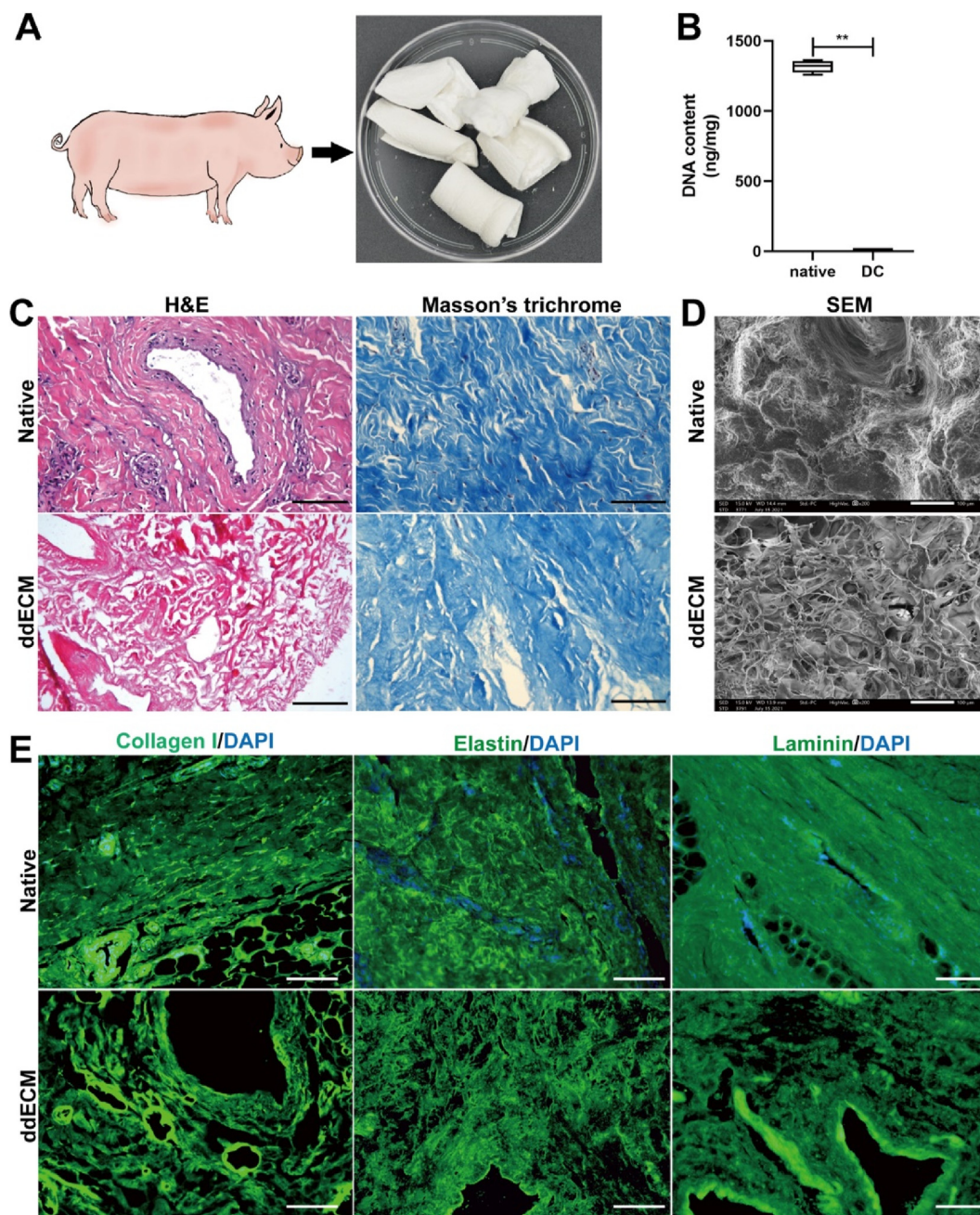
Fig. 1. The characterization of ddECM scaffold. (A) Optical images of ddECM scaffold. (B) DNA content of native dermis and ddECM scaffold. N = 5, *$p < 0.05$, **$p < 0.01$, ***$p < 0.001$. (C) Representative images of H&E staining (left panel) and Masson's trichrome staining (right panel) of native and decellularized dermal tissue. (D) SEM images of native and decellularized dermal tissue. (E) Immunofluorescent staining of native and decellularized dermal tissue. Scale bars: 100 μm.

[16], achieving the accessible sol-gel transition process.

^{1}H NMR spectrum showed the typical signals of acrylamide double bond, which was indispensable for photopolymerization in both ddECMMA and GelMA hydrogels, revealing the successful methacrylation on ddECMMA hydrogel (Fig. 3A and Fig. S1A, Supporting Information). The viscoelastic properties of the ddECMMA hydrogel were measured by a dynamic rotational rheometer, including the mechanical strength and gelling time. A frequency-sweep test was applied for the assessment of storage modulus (G′) of different concentration ddECMMA precursor solution (arranging from 3% to 6%), and the result showed that compared with GelMA hydrogel, 4%, 5% and 6% ddECMMA hydrogels exhibited higher modulus, approximately 239 Pa, 247 Pa and 234 Pa, respectively, among which 5% was highest and increased up to 3-fold

(Fig. 3B). The irradiation of 365 nm ultra violet (UV) on the 5% ddECMMA precursor solution for 40 s made the storage modulus G′ superior to loss modulus G″ (Fig. 3C), resulting in the hydrogel formation, which demonstrated the property of fast gelling of the ddECMMA hydrogel. Additionally, densely packed pores were homogenously distributed in the GelMA and ddECMMA hydrogels with different concentrations (Fig. 3D). The pore size of 5% ddECMMA hydrogel (87 ± 30 μm) was equivalent to GelMA hydrogel (Fig. 3E and Fig. S1B, Supporting Information), which was beneficial for facilitating cellular activities [17]. The degradation experiment showed a delayed degradable rate with an increase of concentration of ddECMMA. Collagenase environment rendered GelMA to completely degrade within 3 days, while the time for 5% ddECMMA complete degradation in collagenase solution hydrogels
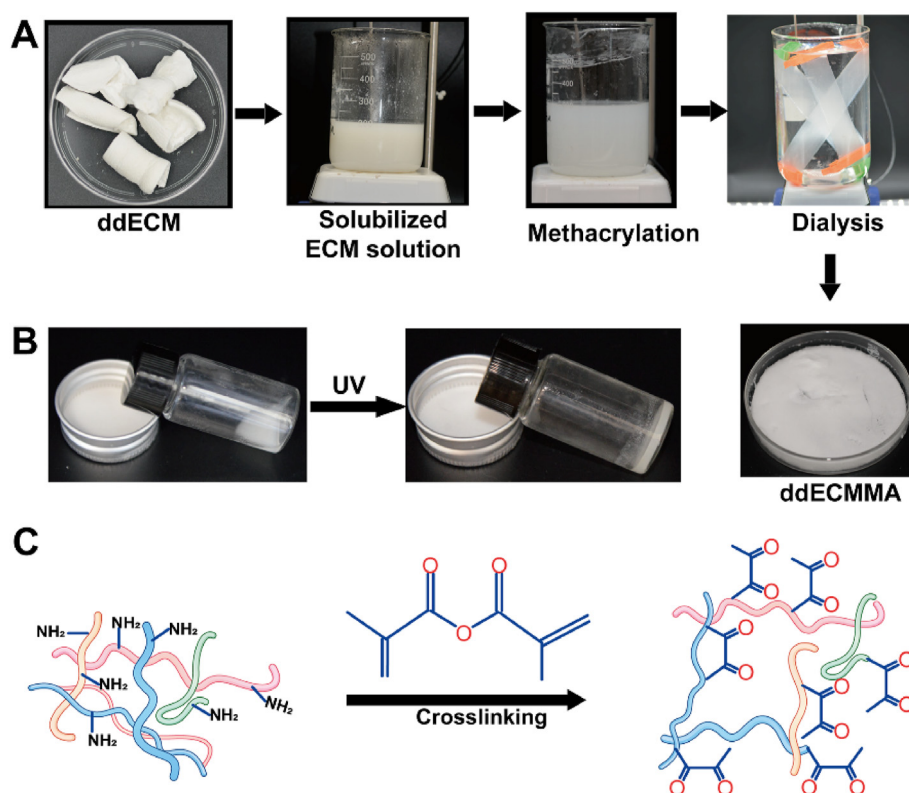
Fig. 2. The preparation of ddECMMA hydrogel. (A) Optical images of the fabrication procedure of ddECMMA hydrogel. (B) Optical images of ddECMMA precursor solution and formation of ddECMMA hydrogel under UV light. (C) Schematic illustration of crosslinking mechanism of the ddECMMA hydrogel.

was extended to 7 days (Fig. 3F). Similarly, the degradable rate of ddECMMA was markedly decreased in PBS environment [14] (Fig. 3G).

As the active elements of ECM, growth factors are the key of ECM-based biomaterials to function biologically [18]. Considering their possible loss during decellularization and methacrylation procedures, we quantified the various growth factors of native dermal tissue, ddECM scaffold and ddECMMA hydrogel using a Growth Factor Microarray. As shown in Fig. 3H, the majority of investigated growth factors and cytokines were retained within the ddECMMA hydrogel, including growth factors promoting wound healing (bFGF, FGF4, FGF6, FGF7, EGF, PDGF-AB, PDGF-BB, TGF-α, TGF-β), growth factors regulating hair follicle cycle (IGF1, IGF2), growth factors regulating the maturation and differentiation of immune cells (CSF1, CSF3), and the neurotrophic growth factor GDNF. It should be noted that HB-EGF, PDGF-AA, VEGF-A and HGF were obviously decreased, compared with the native dermis, while in comparison with the ddECM scaffolds, the contents of these growth factors were no statistically significant. It is widely acknowledged that the capacity of ECM-induced tissue repair and regeneration is mainly attributed to growth factors and cytokines. However, the processes of decellularization and physiochemical modification often lead to the content reduction and disproportion of growth factors, which may alter the outcomes of tissue repair and regeneration. It is a worthy of thorough research issue.

2.2. ddECMMA hydrogel propels cellular activities in vitro

To evaluate the cytotoxicity of ddECMMA hydrogels, we applied the three-dimensional (3D) embedded culture technique to HUVECs (Fig. 4A), and conducted the live/dead staining. This culture system facilitated omni-faceted interactions between cells and hydrogels, so as to provide reliable evidence for cytocompatibility assessment [19]. After 24 h of culture, the Live/Dead staining analysis showed few dead cells on the ddECMMA hydrogels (Fig. 4B), with cell viabilities greater than 90%

and no significant differences from GelMA hydrogel (Fig. 4C), indicating noncytotoxicity of the ddECMMA hydrogels. Additionally, although no statistical differences among the cell viabilities in ddECMMA hydrogels with all concentrations, 5% ddECMMA hydrogel exhibited lower viability than 4% ddECMMA hydrogel. The cytocompatibility of ddECMMA hydrogel was not confined to HUVECs, but extended to other cell type, such as L929 fibroblasts (Fig. S2, Supporting Information). Cell migration was crucial for a biomaterial to facilitate proper regeneration [20] by Z-projection of confocal images stained with phalloidin in the 3D on-top culture system. Compared with other groups, cells cultured in 5% ddECMMA group exhibited higher migration speed, with 3.5-fold, 2.6-fold, 2.4-fold and 1.6-fold of cell migration distance compared with those in GelMA hydrogel, 3% ddECMMA hydrogel, 4% ddECMMA hydrogel, and 6% ddECMMA hydrogel, respectively (Fig. 4D, E). Under the influence of ECM, HUVECs can form three-dimensional capillary-like tubular structure [21]. As exhibited in Fig. 4F, the ddECMMA hydrogel and GelMA hydrogel conducted HUVECs to differentiate and migrate to branch. Mean branch point of HUVECs in GelMA group was 139.6 per field (Fig. 4G). When cultured with ddECMMA hydrogel, the branch point of HUVECs was obviously increased, with the average value of 143, 154.2, 164.3, and 162.5 in 3% ddECMMA hydrogel, 4% ddECMMA hydrogel, 5% ddECMMA hydrogel and 6% ddECMMA hydrogel, respectively. More tubular polygonal networks formed by HUVECs, indicating higher *in vitro* angiogenesis activity of ddECMMA hydrogel. Therefore, on the basis of the above results for the rheological properties and the cellular compatibilities *in vitro* of the ddECMMA hydrogels, we selected the concentration of 5% of ddECMMA hydrogel to the *in vivo* treatment. What's more, ECM has been shown to play a critical role in reepithelialization and angiogenesis during wound healing [22]. Be universally known, ECM is a repository of various GFs, including FGF, EGF, TGF, VEGF and PDGF, in the body [23]. These GFs bind specifically to ECM proteins and are released gradually with the degradation of ECM, stimulate and regulate cellular migration, proliferation and
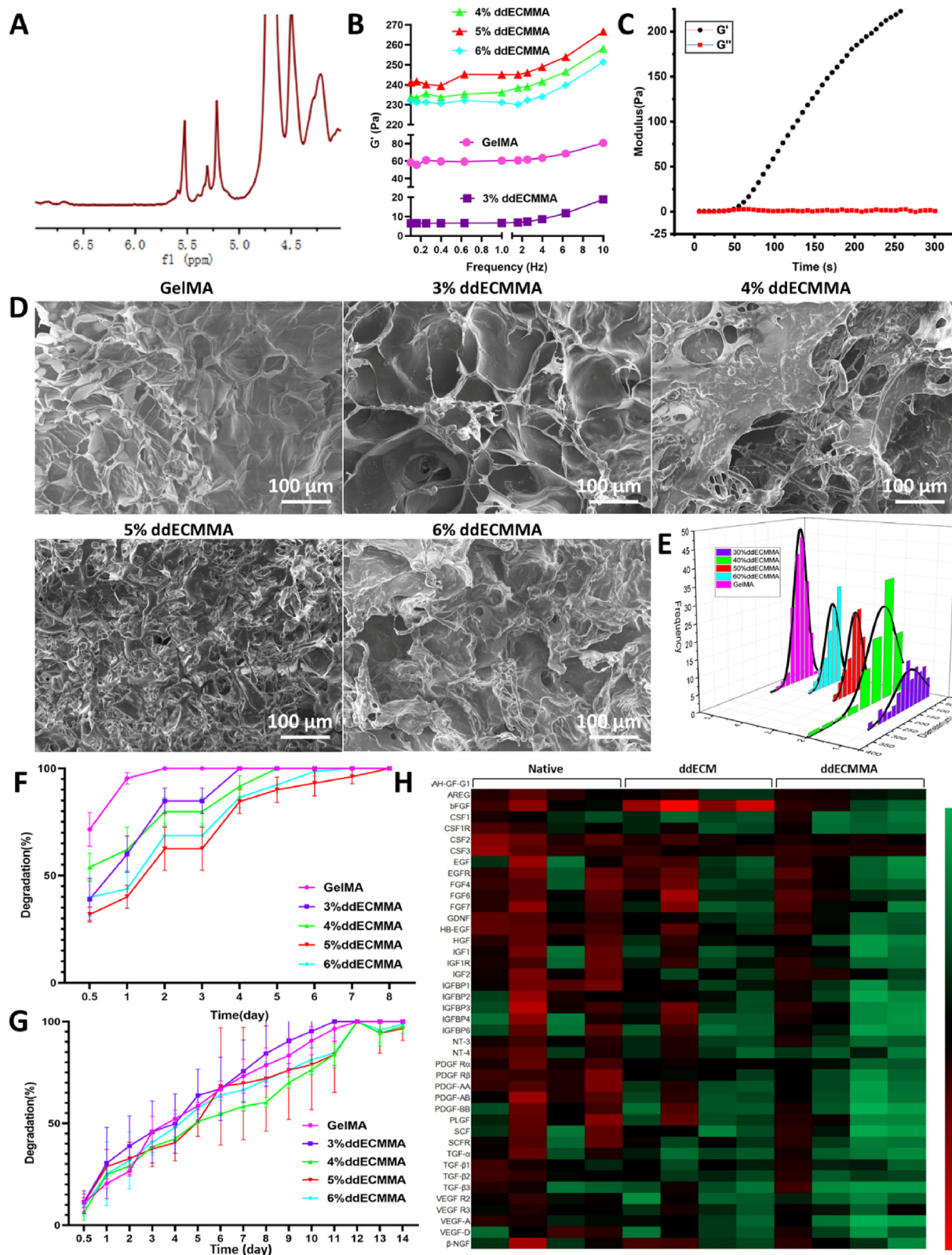
Fig. 3. The characterization of ddECMMA hydrogel. (A) ^{1}H NMR spectrum and (B) Frequency-sweep assessment of storage modulus of different concentration ddECMMA precursor solution (n = 5). (C) Storage modulus (G′) and loss modulus (G″) of 5% ddECMMA. (D) SEM images of ddECMMA hydrogels with different concentration. Scale bars: 100 μm. (E) Quantitative analysis of pore size (n = 3). Degradation rate of different concentration of ddECMMA hydrogels in (F) collagenase and (G) PBS environment (n = 3). (H) Heat map representation of growth factor microarray analysis (n = 4).
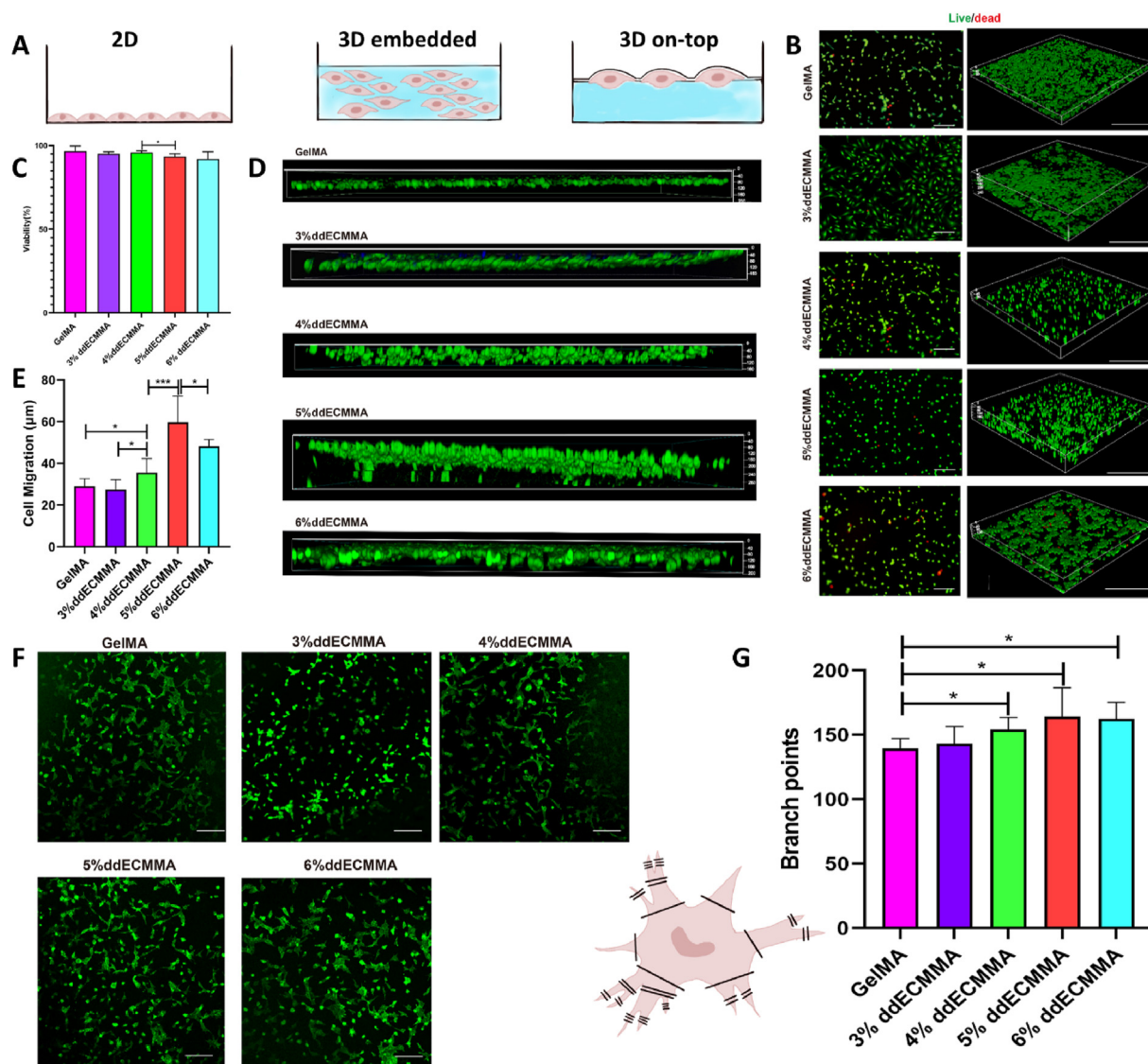
Fig. 4. The ddECMMA hydrogel propels cellular activities *in vitro*. (A) Schematic of HUVECs grown on cell-culture plastic dish (left), in the 3D embedded assay (middle) and in the 3D on-top assay (right). (B) Representative images of live/dead staining. Scale bars: 100 μm (left panel) and 250 μm (right panel). (C) Quantitative analysis of live/dead staining (n = 5). *$p < 0.05$, **$p < 0.01$, ***$p < 0.001$. (D) Z-projection of confocal images stained with phalloidin in the 3D on-top culture system. (E) Quantitative analysis of cell migration speed (n = 7). *$p < 0.05$, **$p < 0.01$, ***$p < 0.001$. (F) Representative images of HUVECs tube formation assay. Scale bars: 100 μm. (G) Quantitative analysis of HUVECs tube formation in terms of the total branch points (n = 5). *$p < 0.05$, **$p < 0.01$, ***$p < 0.001$.

differentiation involved in tissue regeneration and repair, promoting tissue repair, reconstruction and angiogenesis. These different components endowed ECM with various properties, making it an ideal bioactive material for tissue and organ repair and regeneration.

2.3. ddECMMA hydrogel imparts wound healing

We next investigated the effects of ddECMMA hydrogels *in vivo* in a rat excisional wound splinting model [24], and used GelMA hydrogel [25] with the same concentration as the control. Each wound of the ddECMMA- and GelMA-treated groups was administrated with the pre-gel solution, and then exposed under ultraviolet flashlight (365 nm) to induce gelation. To prevent the precursor solution flow around, the pre-gel solution was treated by pre-cooling for 5 min. Gross appearances of wound closure were photographed to document the development of wound healing under different treatments at day 0, 3, 7 and 14 post the surgical procedure (Fig. 5A). The wound sizes in all three groups reduced over time. The wound sizes in all three groups reduced over time, with no

erythema or gross signs of inflammation in wounds. When comparing wound closure to the negative control treatment (no hydrogel, the average rate of 61.9%), GelMA hydrogel induced a more rapid wound closure (assessed on day 7 after wounding), with a healing rate of 78.3%. The dressing of ddECMMA hydrogel propelled the most rapid wound closure, with the healing rate of 84.8% (Fig. 5A and B). As illustrated in Fig. 5C, no significant differences of wound closure rate were noted among the three groups at day 3. Subsequently, at day 7, the wounds in the ddECMMA group displayed a considerable closure than that of the sham- and GelMA-treated wounds, with significant statistical differences ($p = 0.0000019$ and 0.0307, respectively). Moreover, in the late phase (day 14), the use of ddECMMA hydrogel accelerated wound repair, with a 1.2-fold acceleration compared with the other two groups ($p = 0.0032520$ and 0.025143, respectively). Consistent with these results, histological evaluation of the wounds in non-hydrogel rats showed that the epithelium of ddECMMA-treated wounds was longer than that of the other two groups, even on day 7 (Fig. 5D). By day 14, the wound length of ddECMMA-treated wounds became shortest among all the three groups,
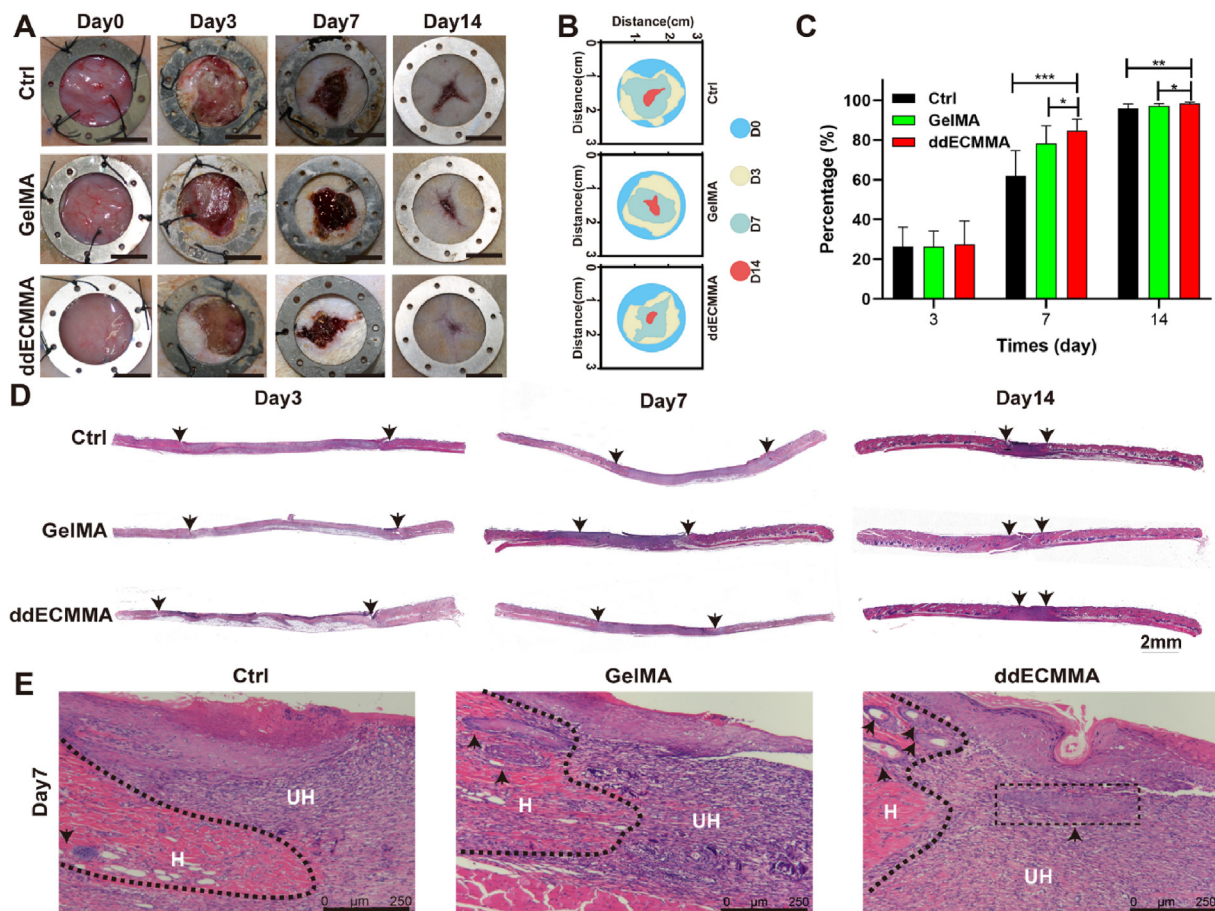
Fig. 5. The ddECMMA hydrogel induces wound healing in rats excisional wound splinting model. (A) Gross images of full-thickness skin defects at day 0, 3, 7 and 14 post-surgeries. Ctrl, control group (without hydrogel). Scale bars: 1 cm. (B) Traces of wound-bed closure during the observed 14 days. (C) The wound closure rates of all three groups (n = 6). *$p < 0.05$, **$p < 0.01$, ***$p < 0.001$. (D) H&E staining of the wounds reveals the re-epithelialization and the unhealed wound length (The unhealed wound edges are outlined by black arrowheads). Scale bars: 2 mm. (E) H&E staining of the edge of wounds at day 7 reveals hair follicle migration. H, healed wounds; UH, unhealed wounds. Scale bars: 250 μm.

indicating that the ddECMMA hydrogel facilitated the rapid closure of wound site that was critical to restore skin barrier function. As shown in Fig. 5E and Figure S3, the histological sections of the wounds without hydrogel displayed some hair follicles and sebaceous glands in the healed tissues, which located near the unhealed wounds, similar to the GelMA treated-wounds. Surprisingly, on day 7 and 14, the hair follicles in the ddECMMA-treated tissues were clealy observed to migrate from healed area into unhealed wounds, indicating a possibility of de novo regeneration.

2.4. Wound healing induced by ddECMMA hydrogel is scarless

Wound healing, a conserved evolutionary process among species, in adult mammals always results in scar formation that lacks appendages, such as hair follicles and sebaceous glands [26]. Hence, the measurement of hair follicles and sebaceous glands is critical to dissect the regenerative phenomenon observed in ddECMMA hydrogel-repaired wounds. Upon hematoxylin and eosin (H&E) staining, hair follicles per field view in ddECMMA group increased up to 2.1-fold compared with that in sham on day 3 (Fig. 6A, B). On day 14, 1.5- and 1.3-fold increases were observed in comparison to the sham and GelMA-treated groups, respectively. While on day 7 ddECMMA hydrogels implantation reduced the number of hair follicles, which may be explained by that the hair follicle growth and migration cannot pursue the high-speeding wound healing. Hair follicle morphogenesis and growth have been verified to depend on the comprehensive cooperation of hair follicle stem cells [27]. As described

by flow cytometry analysis and t-distributed stochastic neighbor embedding (t-SNE) algorithm, hair follicle stem cells induced by ddECMMA hydrogels during wound healing process increased more obviously than that in sham and GelMA-treated wounds (Fig. 6C), and SOX9, which is intensively related to maintaining the characteristics and pluripotency of hair follicle stem cells [28], was expressed positively in parts of hair follicles after injury, as delineated in the control sections in Fig. 6D, a fact that responds to the injury stimulation [27]. The implantation of GelMA hydrogel activated more SOX9$^+$ hair follicle stem cells of hair follicles than the without hydrogel group. By contrast, the ddECMMA-treated wounds boosted the positive expression of SOX9$^+$ hair follicle stem cells in epidermis and hair follicles, mainly the bulge of hair follicles. The existence and release of growth factors, particularly IGF, HGF and VEGF, are thought to be important in the maintenance of hair growth in ddECMMA hydrogels and in the acceleration of hair follicle morphology and circulation [27]. Over time, the positive labelled hair follicle stem cells in all three groups decreased, with relatively few on day 14. In short, the interference of ddECMMA hydrogel prompted the development of hair follicles by activation of SOX9-positive stem cells.

Additionally, collagen organization, in which another major difference between scar formation and scar-free skin regeneration lies [29], was assessed. Masson's trichrome staining showed significantly more collagen deposition in wounds treated with hydrogels (Fig. 7A and B), especially the ddECMMA hydrogel, compared with wounds without hydrogel, at each time point. Notably, in ddECMMA-treated wounds the ratio of collagen type III to type I was 1.7-fold and 2.5-fold higher than in
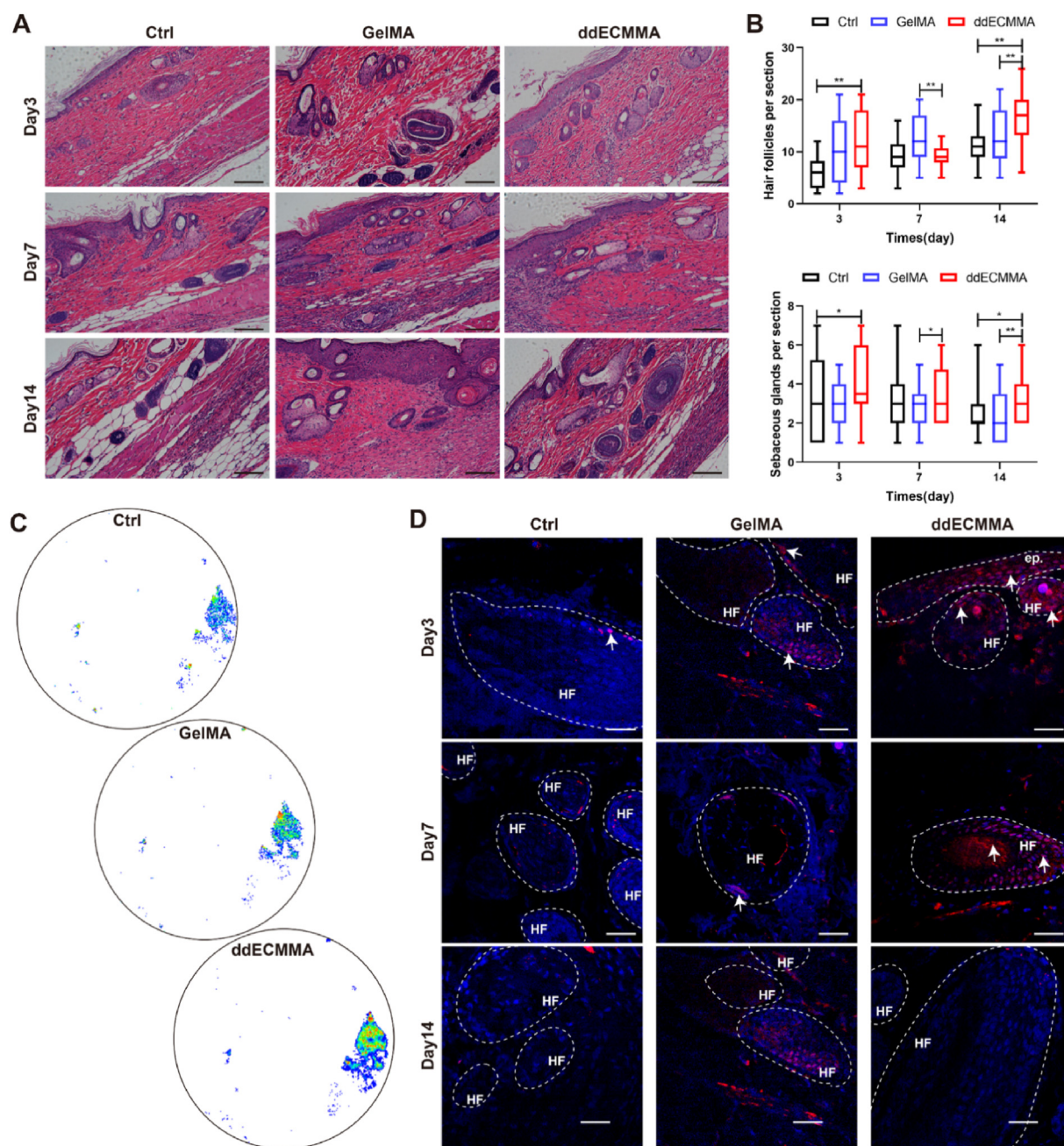
Fig. 6. The ddECMMA hydrogel induces neogenesis of hair follicles in rats full-thickness skin wounds. (A) H&E staining of healed skin wound on each time point reveals the hair follicles and sebaceous glands per field view. Scale bar: 100 μm. (B) Histological quantification of hair follicles and sebaceous glands (n = 20). *$p <$ 0.05, **$p <$ 0.01, ***$p <$ 0.001. (C) T-SNE visualization of flow cytometry data of CK15 and P63 expression in control, GelMA and ddECMMA wounds. (D) Immunofluorescent staining of SOX9 (red) reveals the SOX9-positive hair follicle stem cells (white arrowheads) within hair follicles and epidermis (outlined by white dashed lines). HF, hair follicles; ep., epidermis. Scale bars: 100 μm. (For interpretation of the references to colour in this figure legend, the reader is referred to the Web version of this article.)

the sham and GelMA-treated tissues during the early process of wound healing, respectively (Fig. 7C and D and Fig. S4, Supporting Information). The rapid rate of collagen synthesis and high ratio of collagen III to I induced by ddECMMA hydrogel is consistent with the collagen organization in fetal scarless wound healing [29a], thus confirming that the scarless of wound healing by ddECMMA.

2.5. ddECMMA hydrogel enhances angiogenesis in vivo

The success of skin regeneration depends on an efficient vascularization process that delivers adequate nutrients, growth factors and

oxygen for tissue regeneration and releases paracrine signals that regulate the growth, differentiation and regeneration of various cells [30]. To evaluate the vascularization potential of ddECMMA hydrogel, micro-computed tomography (micro-CT) combined with the injection of radiopaque contrast agents was performed. As shown in Fig. 8A and B, the micro-CT scanning images displayed that the vascular architecture of the ddECMMA wounds was hierarchical with increased vessel volume by comparison with the non-hydrogel-treated and GelMA-treated wounds on day 7 and 14. Quantitative analysis showed that the mean vessel diameter decreased over time in non-hydrogels and ddECMMA hydrogels, which reflected that blood vessels gave off fine capillary tributaries
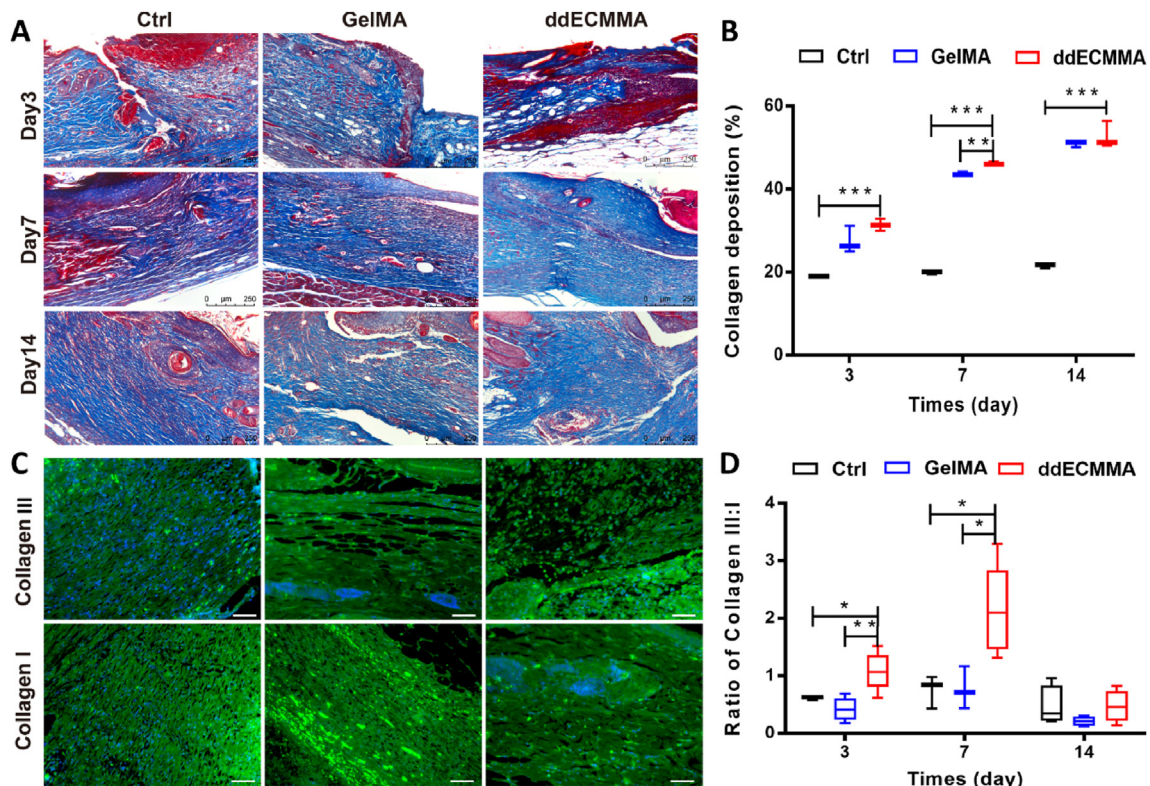
Fig. 7. Collagen organization in the repaired wounds. (A) Masson's trichrome staining illustrates the fibers distribution. Blue, collagen fibers; red, muscle fibers. Scale bars: 250 μm. (B) Histological quantification of collagen deposition (n = 5). *$p < 0.05$, **$p < 0.01$, ***$p < 0.001$. (C) Immunostaining for collagen III (green, upper line) and collagen I (green, lower line). Scale bars: 100 μm. (D) Quantitative analysis of the ratio of collagen III to I (n = 5). *$p < 0.05$, **$p < 0.01$, ***$p < 0.001$. (For interpretation of the references to colour in this figure legend, the reader is referred to the Web version of this article.)

(Fig. 8C), suggesting that ddECMMA hydrogel induced a highly functional angiogenic response. Histologically, the immunofluorescent staining of CD31 and α-SMA, respectively revealing vascular endothelial cells and pericytes, showed large amount of CD31-stained endothelial cells in the early stage of wound healing in the ddECMMA group, increased CD31-positive endothelial cells on day 7, reflecting a rapid endothelial cell response and a robust capillary growth (Fig. 8D, E). While on day 14, CD31-labelled vessels decreased, which can be attributed to that some of the newly formed capillaries regress, followed by vessel maturation to bring nutrients, immune cells, and oxygen to healing wounds. The enhanced vascular recruitment by ECM hydrogels can be explained through several mechanisms. Firstly, ECM hydrogels can provide a scaffold structure that offers physical support for the formation of new blood vessels. These hydrogels can mimic the extracellular matrix (ECM), providing the necessary mechanical support and cell adhesion signals to facilitate the settlement and proliferation of endothelial cells in the wound area. Additionally, the bioactive components present in ECM hydrogels, such as ECM proteins, growth factors, and intercellular signaling molecules, can promote vascular recruitment by directly or indirectly modulating signaling pathways associated with angiogenesis. An important mechanism is the activation of signaling pathways in endothelial cells and vascular smooth muscle cells by growth factors and ECM proteins present in ECM hydrogels, which promote blood vessel formation and remodeling. These growth factors may include vascular endothelial growth factor (VEGF), platelet-derived growth factor (PDGF), and fibronectin, among others. By releasing these growth factors, ECM hydrogels can stimulate endothelial cell migration and proliferation and induce undifferentiated cells to differentiate into vascular smooth muscle cells, thereby facilitating angiogenesis and maturation.

2.6. ddECMMA hydrogel elicits macrophage-predominated immunomodulation

Remarkable advances in research have shown that the immunomodulatory role performed by immune cells is one of the key mechanisms of tissue repair and regeneration, determining the extent of scar formation and the recovery of tissue structure and function [31]. To further explore the immunomodulatory mechanisms instrumental in triggering the activation of scarless wound healing, we conducted multi-parameter flow cytometry staining and performed unsupervised clustering with t-SNE. As depicted in Fig. 9A and B and Fig. S5, on day 3, the late stage of inflammation, the control groups detected scarce CD45$^+$CD86$^+$CD206$^+$ (M2) cells, while the ddECMMA-treated wounds presented approximately 3.4-fold higher percentage of M2 macrophages (Fig. 9A and B), which is distinct from M1 macrophage polarization stimulated by decellularized dermal scaffold [32]. Immunofluorescence analysis of wound sections obtained at day 3 showed heavily infiltrated with CD163-positive cells within ddECMMA-implanted wounds compared with controls, verifying increased quantities of anti-inflammatory M2 macrophages (Fig. 9C). Noteworthy is that, besides M2 macrophages, T helper 1 cells (Th1) and natural killer cells (NK) were elicited in the presence of ddECMMA hydrogel on day 3 (Fig. 9A and B and Fig. S5, Supporting Information). Considering that these two cell types are not associated with type 2 immune responses resulting wound repair and tissue regeneration [33], we did not conduct in-depth study. While further studies are needed to validate the role of these two cells in the ddECMMA hydrogel-mediated scar-free wound healing. On day 14, large number of macrophages underwent apoptosis (that is, programmed cell death), and exited from the wounds. Meanwhile, the up-regulation of M2 macrophages induced by ddECMMA hydrogel in the
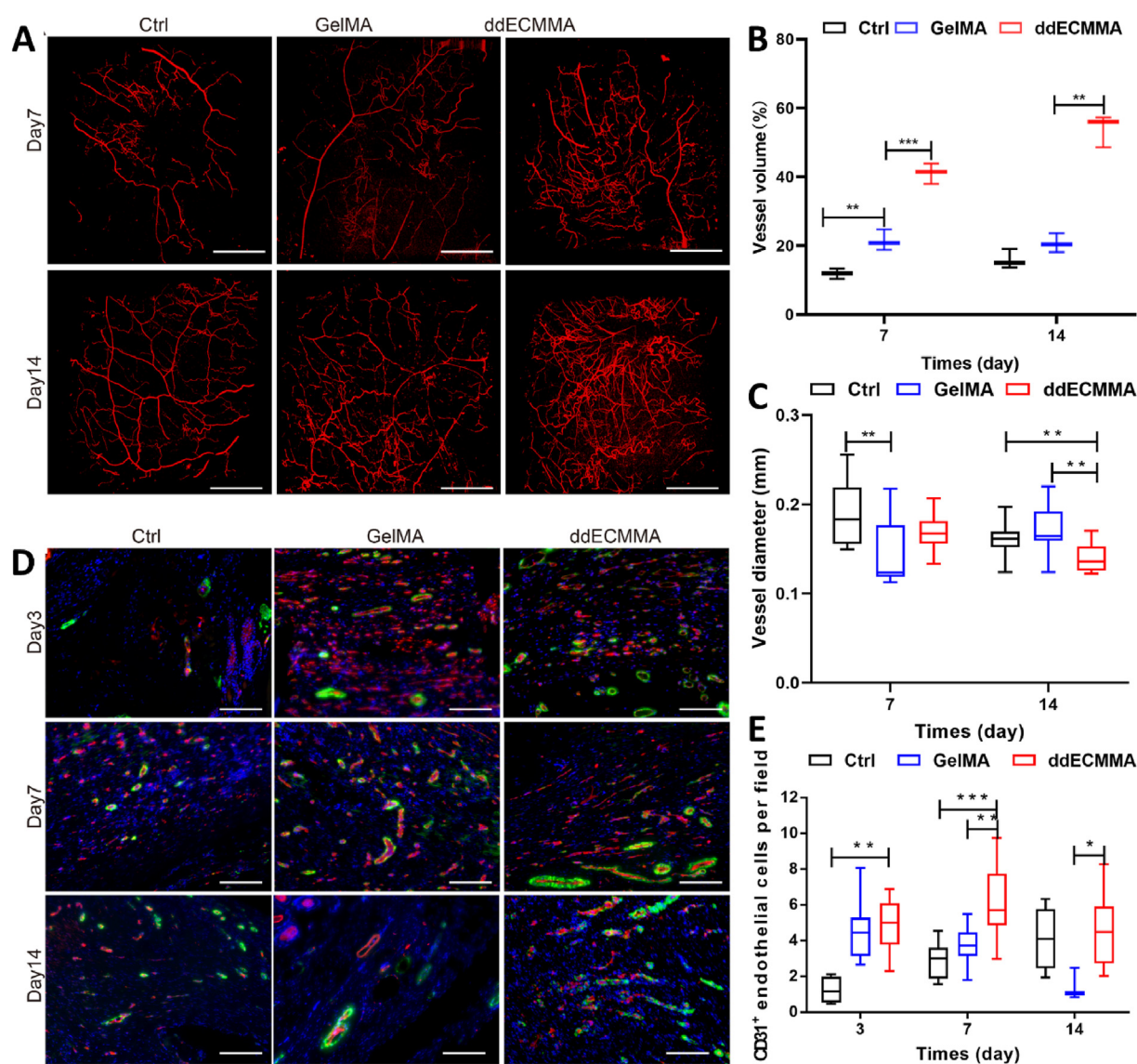
Fig. 8. The ddECMMA hydrogel enhances angiogenesis during scarless wound healing. (A) Micro-CT scanning images of the architecture of functional vessels on day 7 and day 14 post-operation. Scale bars: 5 mm. (B) Quantitative analysis of vessel volume (n = 3) and (C) vascular diameter (n = 16). $*p < 0.05$, $**p < 0.01$, $***p < 0.001$. (D) Immunostaining of CD31 (red) and α-SMA (green) in control, GelMA and ddECMMA wounds. Scale bars: 100 μm. (E) Quantification of CD31-positive endothelial cells per field. $*p < 0.05$, $**p < 0.01$, $***p < 0.001$. (For interpretation of the references to colour in this figure legend, the reader is referred to the Web version of this article.)

early stage of wound healing was confirmed by RT-PCR results. The expressions of M2 macrophages markers (*Arginase1* and *Fizz-1*) on day 3 and 7 increased in response to the implantation of ddECMMA hydrogel (Fig. 9D and E), compared with controls. During wound healing process, macrophages infiltrated into the wound site are polarized towards M1 phenotype with phagocytic and clearance properties, followed by a transition from M1 subtype to M2 subtype, which was an essential prerequisite for successful wound healing [34]. As shown in Fig. 9C and F, the M2/M1 ratio in ddECMMA hydrogel group was significantly higher than those in control groups, indicating that ddECMMA hydrogel activated a smooth M1-to-M2 transition of macrophages in the early phase of wound healing.

Anti-inflammatory macrophages (M2) facilitate wound healing by producing series of closely related growth factors, supported by accumulated researches [35]. Notably shown in Fig. 9G, the gene expressions of *Fgf2* and *Igf1* were obviously up-regulated on day 3 by ddECMMA hydrogel implantation, and down-regulated on day 7 and day 14. The time-dependent regulation of growth factors displayed to be correlated

with the timed activation of hair follicle stem cells (Fig. 6D). Collectively, our results revealed that the rapid M1-to-M2 transition and the enhanced pro-regenerative microenvironment are the key mediators in scar-free wound healing elicited by ddECMMA hydrogel.

3. Conclusion

In summary, a porcine dermal-derived ddECMMA hydrogel was constructed by covalent crosslink reaction with methacrylic anhydride and amino groups within the ddECM, with abundant biological active cues, tailorably physiochemical property, excellent rheology property and high cell viability. By applying to repair critical-sized full-thickness skin defect, we demonstrated that the ddECMMA hydrogel activated SOX9-positive hair follicle stem cells, prompted the development of hair follicles and facilitated scar-free wound healing coupled with obviously elevated angiogenesis. More intriguingly, the ddECMMA hydrogel could accelerate the M1-to-M2 macrophage transition and up-regulate growth factors to mobilize a pro-regenerative microenvironment and promote
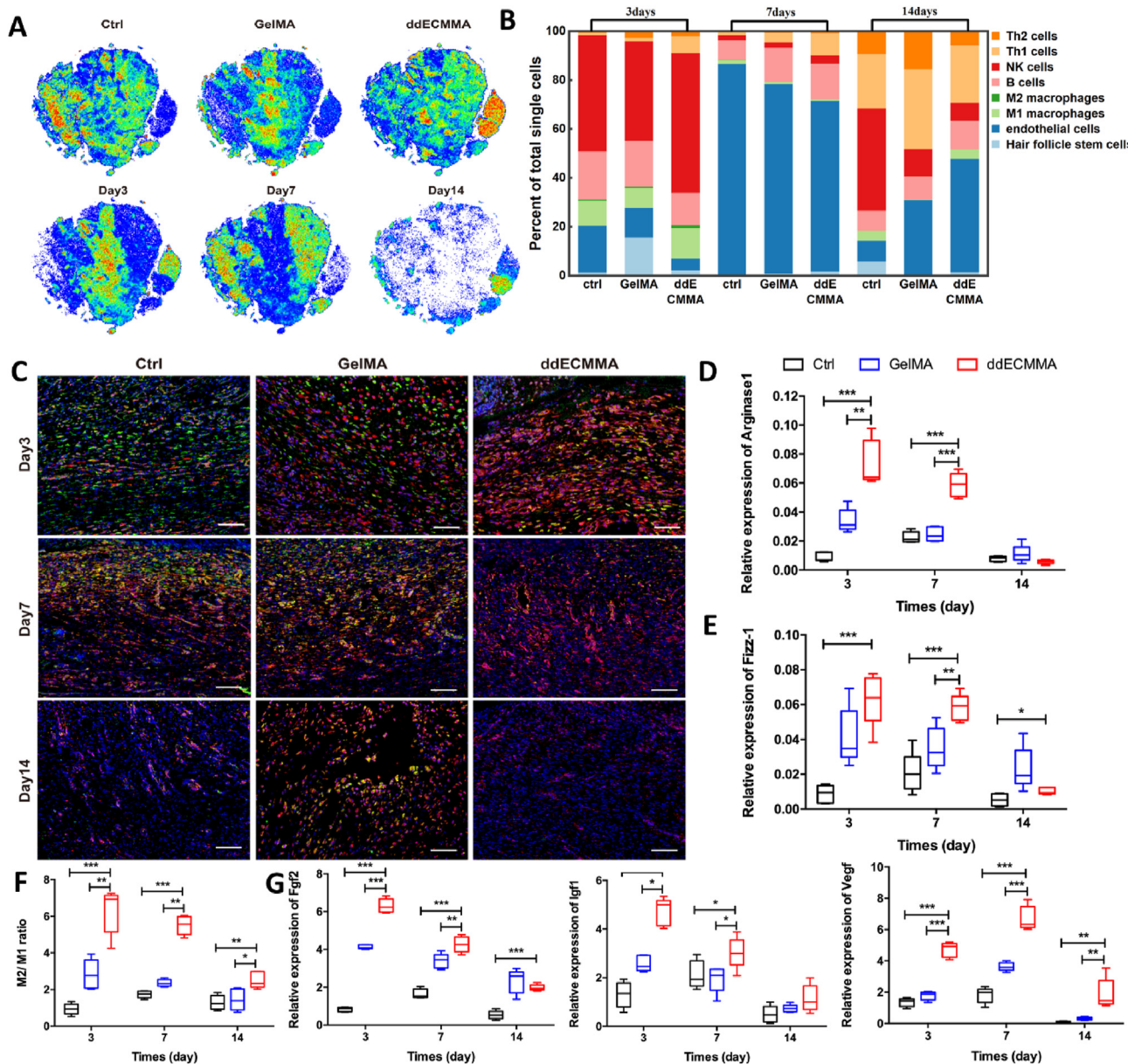
Fig. 9. The immunomodulatory effect of ddECMMA hydrogel in prompting scar-free wound healing. (A) T-SNE visualization of multi-parameter flow cytometry data. (B) Flow cytometric analysis. (C) Representative immunofluorescent staining for iNOS (green) and CD163 (red). Scale bars, 100 μm. (D–E) RT-PCR for the expression of Arginase1 (D) and Fizz-1 (E) in wounds (n = 3). *$p < 0.05$, **$p < 0.01$, ***$p < 0.001$. (F) Quantification of the M2/M1 ratio per tissue observed in the skin wounds. N = 3. *$p < 0.05$, **$p < 0.01$, ***$p < 0.001$. (G) RT-PCR of growth factors (n = 3). *$p < 0.05$, **$p < 0.01$, ***$p < 0.001$. (For interpretation of the references to colour in this figure legend, the reader is referred to the Web version of this article.)

the scar-free skin regeneration. We envision that such biomimetic hydrogels will allow more precise environmental control and multifunctional improvements to support improved skin regeneration.

Credit author statement

Yaling Yu: Conceptualization, Investigation, Methodology, Validation, Writing-original draft. **Huimin Xiao:** Conceptualization, Investigation, Methodology, Validation, Writing-original draft. **Guoke Tang:** Conceptualization, Investigation, Methodology, Validation. **Hongshu Wang:** Conceptualization, Investigation, Methodology, Validation. **Junjie Shen:** Investigation, Methodology. **Yi Sun:** Investigation, Methodology. **Shuaiqun Wang:** Investigation, Methodology. **Wei Kong:** Investigation, Methodology. **Yimin Chai:** Validation, Conceptualization, Funding acquisition, Supervision. **Xuanzhe Liu:** Conceptualization, Supervision, Writing-review & editing. **Xing Wang:** Conceptualization, Supervision, Writing-review & editing. **Gen Wen:** Conceptualization, Supervision, Writing-review & editing.

Experimental section

Detailed experimental section can be found in the Supporting Information.

Declaration of competing interest

The authors declare that they have no known competing financial interests or personal relationships that could have appeared to influence the work reported in this paper.

Data availability

Data will be made available on request.

Appendix A. Supplementary data

Supplementary data to this article can be found online at https://doi.org/10.1016/j.mtbio.2023.100725.

References

[1] a) K. Vig, A. Chaudhari, S. Tripathi, S. Dixit, R. Sahu, S. Pillai, V.A. Dennis, S.R. Singh, Int. J. Mol. Sci. (2017) 18;
b) M. Rodrigues, N. Kosaric, C.A. Bonham, G.C. Gurtner, Physiol. Rev. 99 (2019) 665.
[2] G.C. Gurtner, S. Werner, Y. Barrandon, M.T. Longaker, Nature 453 (2008) 314.
[3] R. Li, K. Liu, X. Huang, D. Li, J. Ding, B. Liu, X. Chen, Adv Sci (Weinh) 9 (2022) e2105152.
[4] a) A.L. Moore, C.D. Marshall, L.A. Barnes, M.P. Murphy, R.C. Ransom, M.T. Longaker, Wiley Interdiscip Rev Dev Biol 7 (2018);
b) Z. Zheng, X. Zhang, C. Dang, S. Beanes, G.X. Chang, Y. Chen, C.S. Li, K.S. Lee, K. Ting, C. Soo, Am. J. Pathol. 186 (2016) 2824;
c) K.L. Lin, D.W. Zhang, M.H. Macedo, W.G. Cui, B. Sarmento, G.F. Shen, Adv. Funct. Mater. 29 (2019) 16.
[5] a) J. Li, C. Zhou, C. Luo, B. Qian, S. Liu, Y. Zeng, J. Hou, B. Deng, Y. Sun, J. Yang, Q. Yuan, A. Zhong, J. Wang, J. Sun, Z. Wang, Theranostics 9 (2019) 5839;
b) Y. Shen, G. Xu, H. Huang, K. Wang, H. Wang, M. Lang, H. Gao, S. Zhao, ACS Nano 15 (2021) 6352;
c) E.Y. Jeon, B.H. Choi, D. Jung, B.H. Hwang, H.J. Cha, Biomaterials 134 (2017) 154.
[6] a) X. Zhang, X. Chen, H. Hong, R. Hu, J. Liu, C. Liu, Bioact. Mater. 10 (2022) 15;
b) S. Kim, S. Min, Y.S. Choi, S.H. Jo, J.H. Jung, K. Han, J. Kim, S. An, Y.W. Ji, Y.G. Kim, S.W. Cho, Nat. Commun. 13 (2022) 1692.
[7] R. Yu, H. Zhang, B. Guo, Nano-Micro Lett. 14 (2021) 1.
[8] a) Y.L. Yu, H.M. Cui, C. Zhang, D.M. Zhang, J. Yin, G. Wen, Y.M. Chai, J. Mater. Chem. B 8 (2020) 4067;
b) Y.L. Yu, H.M. Cui, C. Chen, G. Wen, J. Xu, B.B. Zheng, J.S. Zhang, C.Y. Wang, Y.M. Chai, J. Mei, Biomaterials 165 (2018) 48;
c) Y.L. Yu, H.M. Cui, D.M. Zhang, B. Liang, Y.M. Chai, G. Wen, J. Tissue Eng. Regenerat. Med. 13 (2019) 1770;
d) Y.L. Yu, Y.K. Shao, Y.Q. Ding, K.Z. Lin, B. Chen, H.Z. Zhang, L.N. Zhao, Z.B. Wang, J.S. Zhang, M.L. Tang, J. Mei, Biomaterials 35 (2014) 6822;
e) R. Zhang, J.Q. Jiang, Y.L. Yu, F.F. Wang, N.N. Gao, Y.J. Zhou, X.L. Wan, Z.B. Wang, P. Wei, J. Mei, Bioact. Mater. 6 (2021) 2187.
[9] W. Kim, H. Lee, J. Lee, A. Atala, J.J. Yoo, S.J. Lee, G.H. Kim, Biomaterials 230 (2020) 119632.
[10] a) Z.Y. Chen, B.W. Zhang, J. Shu, H.Y. Wang, Y.D. Han, Q. Zeng, Y.B. Chen, J.F. Xi, R. Tao, X.T. Pei, W. Yue, Y. Han, J. Biomed. Mater. Res., Part A 109 (2021) 1418;
b) C.M. Hsieh, W. Wang, Y.H. Chen, P.S. Wei, Y.H. Liu, M.T. Sheu, H.O. Ho, Pharmaceutics 12 (2020) 18;
c) C. Wang, G.Y. Li, K.G. Cui, Z.H. Chai, Z.Y. Huang, Y. Liu, S. Chen, H.Y. Huang, K.Y. Zhang, Z.B. Han, Y.H. Li, G.L. Yu, Z.C. Han, N. Liu, Z.J. Li, Acta Biomater. 122 (2021) 199.
[11] a) Q. Zhang, C.W. Chang, C.Y. Qian, W.S. Xiao, H.J. Zhu, J. Guo, Z.B. Meng, W.G. Cui, Z.L. Ge, Acta Biomater. 125 (2021) 197;
b) A.M. Jorgensen, Z.S. Chou, G. Gillispie, S.J. Lee, J.J. Yoo, S. Soker, A. Atala, Nanomaterials (2020) 10.
[12] A. Summerfield, F. Meurens, M.E. Ricklin, Mol. Immunol. 66 (2015) 14.
[13] X. Lin, B. Kong, Y. Zhu, Y. Zhao, Adv. Sci. 9 (2022) e2201226.
[14] J. Mao, Q. Saiding, S. Qian, Z. Liu, B. Zhao, Q. Zhao, B. Lu, X. Mao, L. Zhang, Y. Zhang, X. Sun, W. Cui, Smart Med. 1 (2022) e20220005.
[15] J.W. Shin, S.H. Kwon, J.Y. Choi, J.I. Na, C.H. Huh, H.R. Choi, K.C. Park, Int. J. Mol. Sci. 20 (2019).
[16] C.G. Williams, A.N. Malik, T.K. Kim, P.N. Manson, J.H. Elisseeff, Biomaterials 26 (2005) 1211.
[17] G. Bao, T. Jiang, H. Ravanbakhsh, A. Reyes, Z. Ma, M. Strong, H. Wang, J.M. Kinsella, J. Li, L. Mongeau, Mater. Horiz. 7 (2020) 2336.
[18] K.Y. Kulebyakin, P.P. Nimiritsky, P.I. Makarevich, Front. Endocrinol. 11 (2020) 384.
[19] G.Y. Lee, P.A. Kenny, E.H. Lee, M.J. Bissell, Nat. Methods 4 (2007) 359.
[20] P. Zarrintaj, M. Khodadadi Yazdi, M. Youssefi Azarfam, M. Zare, J.D. Ramsey, F. Seidi, M. Reza Saeb, S. Ramakrishna, M. Mozafari, Tissue Eng. 27 (2021) 821.
[21] I. Arnaoutova, H.K. Kleinman, Nat. Protoc. 5 (2010) 628.
[22] a) P. Simon-Assmann, G. Orend, E. Mammadova-Bach, C. Spenle, O. Lefebvre, Int. J. Dev. Biol. 55 (2011) 455;
b) V. Iorio, L.D. Troughton, K.J. Hamill, Adv. Wound Care 4 (2015) 250.
[23] A.R. Murphy, A. Laslett, C.M. O'Brien, N.R. Cameron, Acta Biomater. 54 (2017) 1.
[24] X. Wang, J. Ge, E.E. Tredget, Y. Wu, Nat. Protoc. 8 (2013) 302.
[25] B.J. Klotz, D. Gawlitta, A. Rosenberg, J. Malda, F.P.W. Melchels, Trends Biotechnol. 34 (2016) 394.
[26] M. Takeo, W. Lee, M. Ito, Cold Spring Harb Perspect Med 5 (2015) a023267.
[27] S. Ji, Z. Zhu, X. Sun, X. Fu, Signal Transduct. Targeted Ther. 6 (2021) 66.
[28] N. He, Z. Dong, D. Tai, H. Liang, X. Guo, M. Cang, D. Liu, Cytotechnology 70 (2018) 1155.
[29] a) H. Pratsinis, E. Mavrogonatou, D. Kletsas, Adv. Drug Deliv. Rev. 146 (2019) 325;
b) S. Mascharak, H.E. desJardins-Park, M.F. Davitt, M. Griffin, M.R. Borrelli, A.L. Moore, K. Chen, B. Duoto, M. Chinta, D.S. Foster, A.H. Shen, M. Januszyk, S.H. Kwon, G. Wernig, D.C. Wan, H.P. Lorenz, G.C. Gurtner, M.T. Longaker, Science (2021) 372.
[30] L.A. DiPietro, J. Leukoc. Biol. 100 (2016) 979.
[31] B. Zhang, Y. Su, J. Zhou, Y. Zheng, D. Zhu, Adv. Sci. (Weinh) 8 (2021) e2100446.
[32] J.L. Dziki, D.S. Wang, C. Pineda, B.M. Sicari, T. Rausch, S.F. Badylak, J. Biomed. Mater. Res. 105 (2017) 138.
[33] R.L. Gieseck 3rd, M.S. Wilson, T.A. Wynn, Nat. Rev. Immunol. 18 (2018) 62.
[34] Y. Yu, W. Zhang, X. Liu, H. Wang, J. Shen, H. Xiao, J. Mei, Y. Chai, G. Wen, Compos. B Eng. 230 (2022) 109524.
[35] a) S.Y. Chu, C.H. Chou, H.D. Huang, M.H. Yen, H.C. Hong, P.H. Chao, Y.H. Wang, P.Y. Chen, S.X. Nian, Y.R. Chen, L.Y. Liou, Y.C. Liu, H.M. Chen, F.M. Lin, Y.T. Chang, C.C. Chen, O.K. Lee, Nat. Commun. 10 (2019) 1524;
b) N. Jain, J. Moeller, V. Vogel, Annu. Rev. Biomed. Eng. 21 (2019) 267.